Journal of Computer-Aided Molecular Design, **14:** 611–629, 2000.
KLUWER/ESCOM

Steroid binding by antibodies and artificial receptors: Exploration of theoretical methods to determine the origins of binding affinities and specificities

Sandra Handschuh[a], Bernd Goldfuss[b], Jiangang Chen[b], Johann Gasteiger[a,*] & K.N. Houk[b,*]
[a]*Computer-Chemie-Centrum, Institut für Organische Chemie, Universität Erlangen-Nürnberg, Nägelsbachstrasse 25, D-91052 Erlangen, Germany;* [b]*University of California Los Angeles, Department of Chemistry and Biochemistry, 405 Hilgard Avenue, Los Angeles, CA 90095-1569, U.S.A.*

Received 7 October 1999; Accepted 17 April 2000

Key words: antibody, artificial receptors, free energy calculations, Kohonen neural networks, ligand-receptor binding, molecular similarity

Summary

Binding mode calculations for complexes between an artificial paracyclophane receptor and digoxins, cholic acids as well as cortisone steroids show encapsulation of different ring combinations. Docking experiments were performed between the 26-10 antibody and digoxins. Coordination affinity arises from hydrophobic desolvation and van der Waals interactions rather than from hydrogen bonds. The specificity and affinity arises mainly from shape complementarity. Computed binding free energies and Kohonen neural network computations both point to physicochemical and structural similarities of natural antibodies and artificial receptors.

Introduction

Steroids are involved in many biological functions. The most abundant steroid is the well-known lipophilic cholesterol, **1**, which is both an important component of the cell membrane and has a major function in atherosclerosis. The biosyntheses of steroidal hormones, like glucocorticoids, estrogens or androgens all start from cholesterol [1].

The steroids share the 6-6-6-5 fused ring system and differ by the degree of unsaturation of rings A and B, the number and type of oxygen substituents and the presence or absence of a side chain. Many attempts have been made to find ways to complex steroids. A variety of immune-system-derived [1–3] and artificial receptors are now known which show high binding affinities to steroidal structures [1, 4, 5].

Many antibody steroid complexes have been investigated intensively, e.g., the DB3 progesterone [6], the 26-10, and the 40-50 digoxin, and the 40-50 ouabain complex [7, 8]. Elaborate procedures are necessary to obtain antibodies [9]. Therefore, it is quite advantageous to generate highly specific, tight binding artificial receptors, which can complex steroids and substitute the antibody catalysts for certain cases.

Koga and co-workers first employed artificial cyclophane receptors to complex aromatic steroids [10]. Systematic studies by Diederich et al. using several cyclophanes as artificial receptors revealed a high affinity to various steroid structures [1, 4, 5, 11–13].

Here we explore the nature of receptor-ligand binding using a variety of computational tools. The results provide a better understanding of the interaction mechanisms and give guidance for the design of better receptor systems. Qualitative methods (simulating docking processes, comparison of surface properties using neural networks), as well as quantitative methods (free energy techniques) were applied to analyze steroid binding to both artificial and immune-system-derived receptors.

Using these methods, the binding mode of 26-10 Fab to digoxin **2** and some related steroids [7] and

*To whom correspondence should be addressed. E-mail addresses: houk@chem.ucla.edu; gasteiger@chemie.uni-erlangen.de

the binding mode of paracyclophane **3** to cholic acid **4** steroids [4] have been investigated.

Methods

The structures of all steroids and the cyclophane **3** were minimized with the molecular modeling system MacroModel [14] using the MM3 force field [15]. The sequence of the antibody 26-10 was aligned with known highly homologous antibody structures in order to extract the parts of the light and heavy chain of the entire antibody crystal structure. The ligand binding domain of the antibodies is between the variable light and heavy chain of the peptide. This sequence alignment was performed with the immunoglobin domain modeling program AbM [16].

The steroids were manually predocked into the ligand binding domain of the antibody with the InsightII/Discover [17] software package as well as by analyzing and visual inspection of the results.

Docking experiments to obtain the binding mode of the steroids in the antibody 26-10 and the cyclophane, **3**, cavity were calculated using AutoDock [18]. The charges for the electrostatic grid calculation in AutoDock were obtained from semiempirical PM3 VESPA charges calculated by the molecular modeling package VAMP [19].

The linear interaction calculations to obtain the free energies of binding were performed with a modification of the Amber4.1 package [20] based on the AMBER94 force field [27]. The solvation free energies were simulated for both the guest and the host-guest complex with Jorgensen's TIP3P water box [28]. The average value of the temperature was maintained by means of the Berendsen coupling algorithm [29]. All simulations were performed with a nonbonded cutoff of 10.0 Å. The SHAKE procedure [29, 30] was applied to constrain all bond lengths to their equilibrium values.

The comparisons of molecular surface properties were performed by the self-organizing network of Kohonen [31–34]. The network was used to project three-dimensional molecular surfaces into two-dimensional maps [35–41]. The maps were generated and analyzed by the Kohonen Map Simulator KMAP [42]. The van der Waals surfaces of the three-dimensional structures were calculated using the program SURFACE [43]. Both surface properties, the electrostatic potential and the hydrophobicity, were calculated based on the partial atomic charges of the compounds. These were obtained by the PEOE (Partial Equalization of Orbital Electronegativities) method [44, 45] and its extension to conjugated systems [46].

Hydrophobicity values were obtained from the partition coefficient (log *P*) of the sample in polar/apolar reference systems and the calculation of the Molecular Lipophilicity Potential (MLP) [47, 48].

Two approaches were applied to compare van der Waals surfaces of different molecules [35–40]. The first one is to train several networks, one with each single three-dimensional structure and to align the maps according to structural features which can be recognized in the map. The second method is the template approach [38, 39]. This approach requires an alignment of the molecules of the dataset. The network is then trained once with the data of a template molecule, e.g. the one having the highest activity, and each other structure is sent through this network. At regions of high similarity, colored areas appear on the corresponding map, whereas dissimilar regions are indicated by white areas.

For computational details see Appendix.

Results and discussion

26-10 Fab steroid binding

The crystal structure of the 26-10 Fab-digoxin (**2**) complex was obtained from the Brookhaven Protein Databank (1IGJ) [2]. The structures of the four steroids were taken from Reference 7 (see Figure 1).

First, the binding mode of digoxin, **2**, inside the murine antidigoxin hybridoma 26-10 binding pocket was calculated using AutoDock [18] and compared with the crystal structure of the 26-10 Fab-digoxin complex published by Sheriff and co-workers [2]. Then the binding modes of the steroids digitoxin, **5**, digoxigenin, **6**, and ouabain, **7**, inside the 26-10 binding pocket were determined by AutoDock.

The steroid structures are quite rigid (see Figure 1) with a maximum of 11 exocyclic rotatable bonds for ouabain, **7**. During the AutoDock prediction of docking modes, only the torsion angles of bonds directly attached to the steroid skeleton and the lactone ring were changed. Table 1 gives the bonds that were rotated for each structure during the simulation process.

Each AutoDock run results in several docked configurations of the steroids inside the ligand binding domain of the 26-10 antibody. The lowest energy arrangement of digoxin, **2**, is similar to the crystal

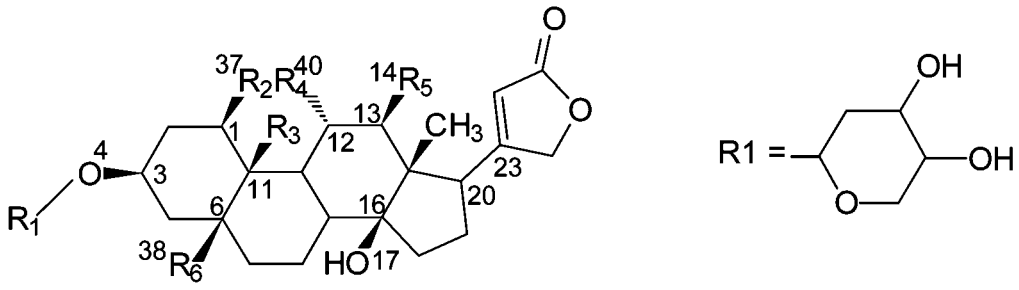

	R1	R2	R3	R4	R5	R6
2 digoxin	sugar	H	CH_3	H	OH	H
5 digitoxin	sugar	H	CH_3	H	H	H
6 digoxigenin	H	H	CH_3	H	OH	H
7 ouabain	sugar	OH	CH_2OH	OH	H	OH

Figure 1. The chemical structures of steroids **2**, **5**, **6**, and **7**.

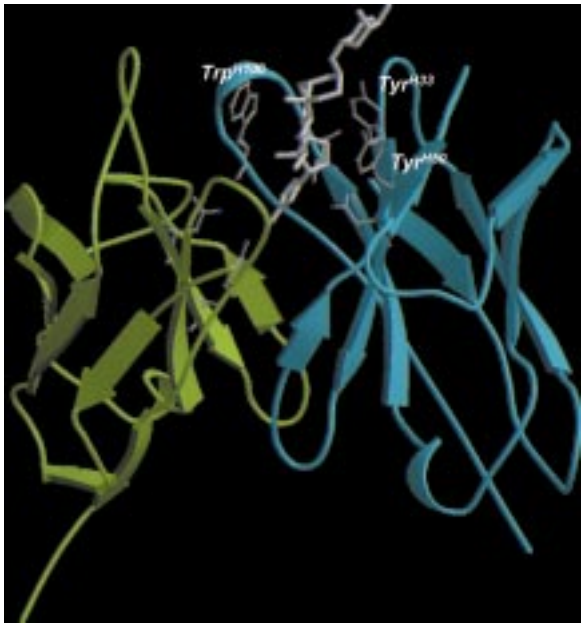

Figure 2. The calculated binding mode of digoxin, **2**, inside the 26-10 antibody binding pocket.

Table 1. List of bonds for each compound which are rotated during the simulated annealing process

	Rotatable bonds
2 digoxin	13–14
	16–17
	20–23
5 digitoxin	16–17
	20–23
6 digoxigenin	13–14
	16–17
	20–23
7 ouabain	1–37
	6–38
	11–21
	12–40
	16–17
	21–39

structure with an average rms value of 0.9 Å. The orientation of the three steroids digitoxin, **5**, digoxigenin, **6**, and ouabain, **7**, inside the binding pocket corresponds closely to the orientation of digoxin, **2**. The lactone substituents on the D-rings of the steroids are buried deepest within the ligand binding sites, and the sugar moiety substituents on the A-rings are exposed to the solvent. The sugar moiety does not contribute to the binding at all (see Figures 2 and 3). The digoxin, **2**, is sandwiched between the aromatic rings of Tyr^{H33}, Tyr^{H50} and Trp^{H100} (see Figures 2 and 3). No hydrogen bonds are formed between any amino acid side

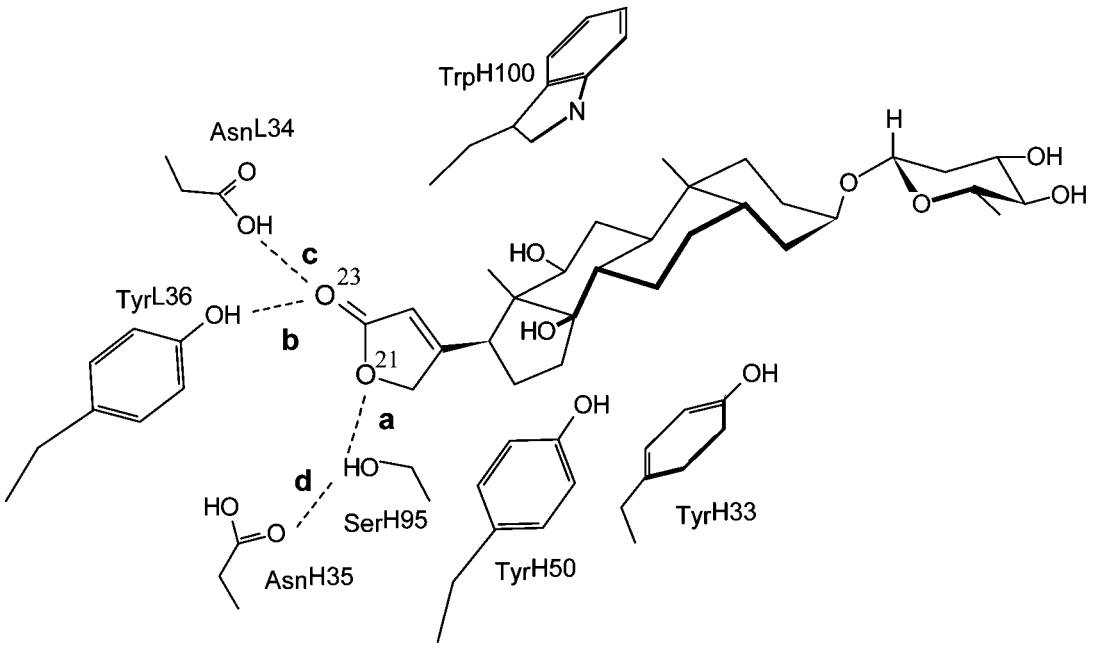

distances:
a ligand O-21 - Ser^{H95} O^{γ}
b ligand O-23 - Tyr^{L36} OH
c ligand O-23 - Asn^{L34} $N^{\delta 2}$
d Ser^{H95} O^{γ} - Asn^{H35} O

	distances [Å]			
	a	**b**	**c**	**d**
crystal structure of **2**	3.55	3.97	4.13	2.84
2 digoxin	3.26	3.60	3.82	2.84
5 digitoxin	3.03	3.83	3.88	2.84
6 digoxigenin	2.93	4.05	4.11	2.84
7 ouabain	3.11	3.83	3.62	2.84

Figure 3. Schematic presentation of the binding site of the 26-10 antibody complexing digoxin, **2**.

chain and the steroids. The only polar groups which are not stabilized by interactions with the solvent or other polar residues are the lactone ring O-21 and O-23 oxygen atoms of the steroids. Although there are potential hydrogen-bond donors in the proximity of O-21, e.g., Ser^{H95} O^{γ}, none of them is close enough to the O-21 of the steroids to form a hydrogen bond except in the case of digoxigenin, **9** (2.93 Å) (see Figure 3). In addition Ser^{H95} O^{γ} already forms a hydrogen bond (2.9 Å) with the side chain amide oxygen of Asn^{H35}. Atom O-23 also makes no hydrogen bonds (see Figure 3).

The AutoDock potential function indicates a van der Waals interaction energy of −50 kcal/mol between digoxin, **2**, and the antibody. 70.4% of these interactions are due to 39.0% of the structure (only including special hydrogens that bind to a non-carbon atom), specifically by the B/C/D-rings and the lactone ring.

The affinity potential of digoxin, **2**, inside the 26-10 fab binding pocket (Figure 4) shows that the largest interactions (> 2.0 kcal/mol) arise from the oxygens of the lactone ring and from the D-ring (colored in red), and parts of the B and C-ring (> 1.5 kcal/mol) (colored in green). The smallest interactions (< 0.5 kcal/mol) are shown by most of the sugar moiety atoms and the ether oxygen (Figure 4: colored in grey). The calculations indicate that 16 atoms are responsible for interactions with the receptor in accordance with the conclusion of Jeffrey et al. [2], where 18 atoms are identified as mostly responsible for the steroid interactions to the antibody ligand binding domain.

The superposition of the crystal structure of digoxin, **2** (red), with the calculated conformations of digoxin, **2** (blue), digitoxin, **5** (green), digoxigenin, **6** (grey), and ouabain, **7** (magenta), in Figure 5 shows the similar orientation of these four steroids inside the binding domain of the 26-10 fab.

The docking experiments showed that the affinity of the steroids to the ligand binding domain of the antibody is based primarily on apolar interactions, although several hydrogen bonds are present as well on the polar lactone head group of the steroid.

Cyclophane steroid binding

To analyze probable binding modes of the steroids in a synthetic cyclophane receptor, AutoDock simulations were performed with **3** as the rigid receptor (like the antibody in the previous section). The structures of the steroids to be docked into this cyclophane cavity and

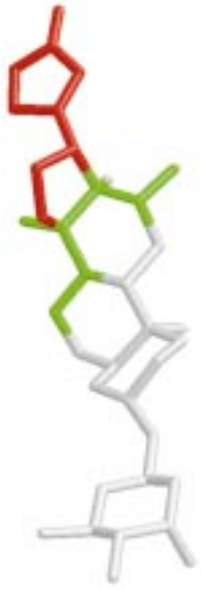

Figure 4. The structural parts of digoxin, **2** which are most responsible for the affinity to the 26-10 antibody binding pocket are marked in red (> 2.0 kcal/mol) and green (> 1.5 kcal/mol).

Figure 5. The superposition of the crystal structure conformation of **2** (red), and the calculated conformations of **2** (blue), **5** (green), **6** (gray), and **7** (magenta).

the cyclophane structure, **3**, were taken from Peterson et al. (see Figure 6) [4].

The most stable conformation of **3** was found by molecular mechanics simulations based on the MM3 force field. In this conformation, the substituents on the benzene rings are blocking the cavity (see top of Figure 7) and hence inhibit steroid encapsulation.

An alternative conformation of **3**, more conclusive to ligand binding, was obtained by additional molecular dynamics calculations on a cyclophane-steroid complex using the MM3 force field. The resulting conformation of **3** (see bottom of Figure 7) was about

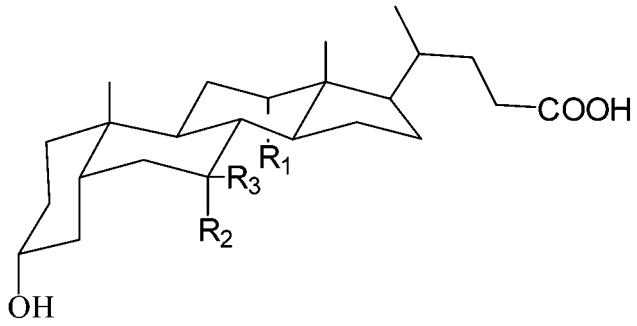

	R1	R2	R3
4 cholic acid	OH	OH	H
8 deoxycholic acid	OH	H	H
9 chenodeoxycholic acid	H	OH	H
10 ursodeoxycholic acid	H	H	OH
11 lithocholic acid	H	H	H

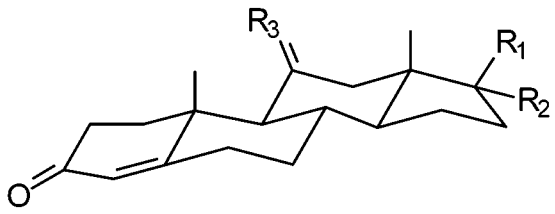

	R1	R2	R3
12 hydrocortisone	$COCH_2OH$	OH	αH, βOH
13 cortisone	$COCH_2OH$	OH	O
14 testosterone	OH	H	H, H
15 progesterone	$COCH_3$	H	H, H

Figure 6. The chemical structures of **4** and **8** to **15**.

21 kcal/mol higher in energy than the global minimum obtained without encapsulated steroid (shown at the top of Figure 7). The less stable, but more open conformation of **3** was used as the ligand binding domain for further calculations.

Docking experiments were performed for the steroids **4** and **8**–**14** (see Figure 6), all of which exhibit a high affinity to the cyclophane receptor [4]. The steroids **2**, **7**, and **15**, which have high affinities to antibody receptors [7, 8] were also docked into the cyclophane binding site. Figures 8–12 show

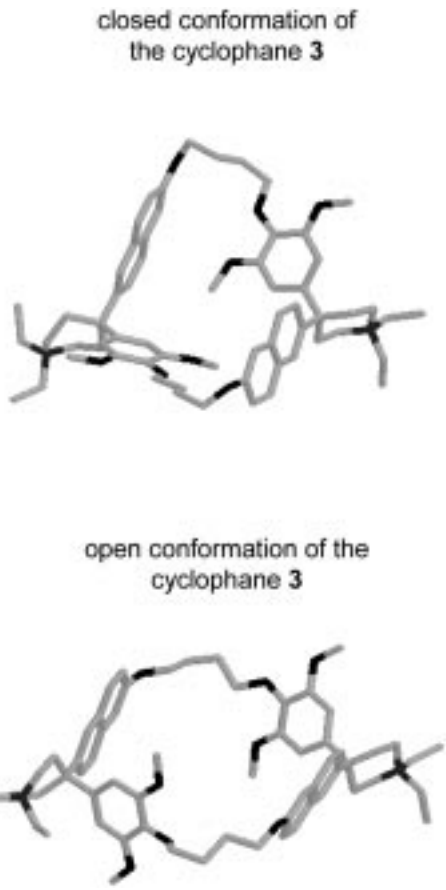

Figure 7. Calculated conformations of **3**; top: without encapsulating a ligand during the molecular dynamics calculations; bottom: encapsulating a ligand during the molecular dynamics calculations.

affinity potentials for the steroid structures **4**, **2**, **7**, and **8**–**15** inside the cyclophane binding site. Those parts of the steroid structures which are mostly responsible for high receptor interactions are displayed in red (total van der Waals interaction energy value $>$ 2.0 kcal/mol) and green (total van der Waals interaction energy value of 1.5 kcal/mol to 2.0 kcal/mol).

Cholic acid, **4**, binds with A ring atoms and B/C/D ring atoms (Figure 8). The α-hydroxy group at the B ring of **4** leads to repulsion (Figure 8), due to the short distance of the hydroxyl hydrogen to the naphthalene moiety in **3** (2.36 Å or 2.92 Å). Deoxycholic acid, **8**, binds in a very similar mode. The same atoms as in **4** contribute in **8** to the highest interactions with the apolar cyclophane cavity (see Figure 8). The interaction energy for **8** is 2.6 kcal/mol higher than for **4**, because of the absence of the unfavorable hydroxy groups at the B-ring in **8**. Chenodeoxycholic acid, **9**, binds with most of the C/D-ring atoms (Figure 8) [49].

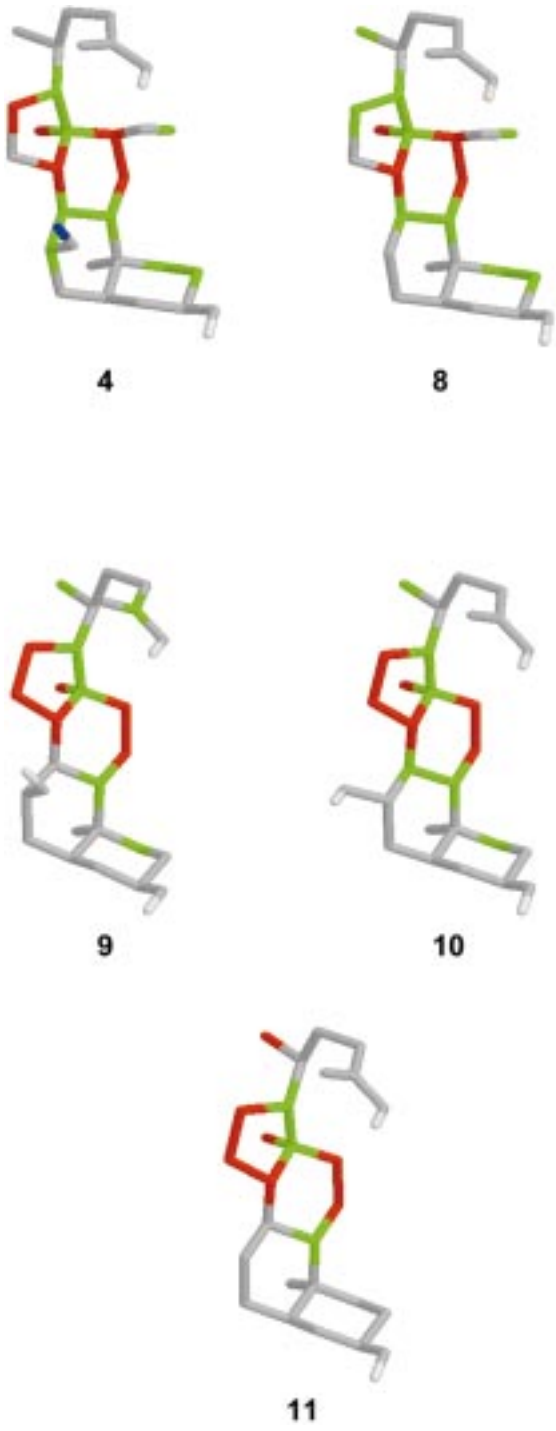

Figure 8. The structural parts of **4** and **8** to **11** which are most responsible for the affinity to the cyclophane, **3**, cavity are marked in red ($>$ 2.0 kcal/mol) and green ($>$ 1.5 kcal/mol). The blue atom of **4** leads to a repulsion.

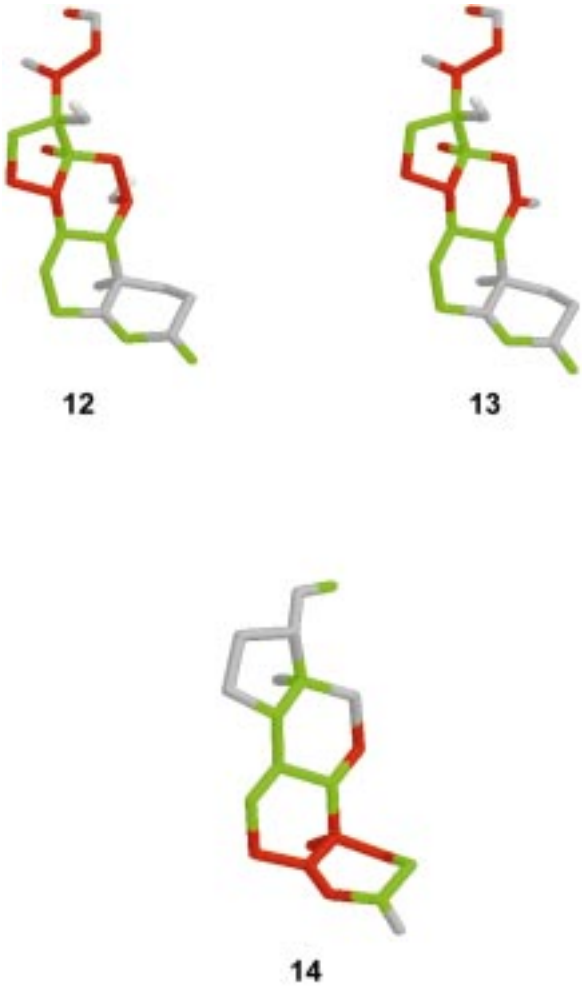

Figure 9. The structural parts of **12** to **14** which are most responsible for the affinity to the cyclophane, **3**, cavity are marked in red (> 2.0 kcal/mol) and green (> 1.5 kcal/mol).

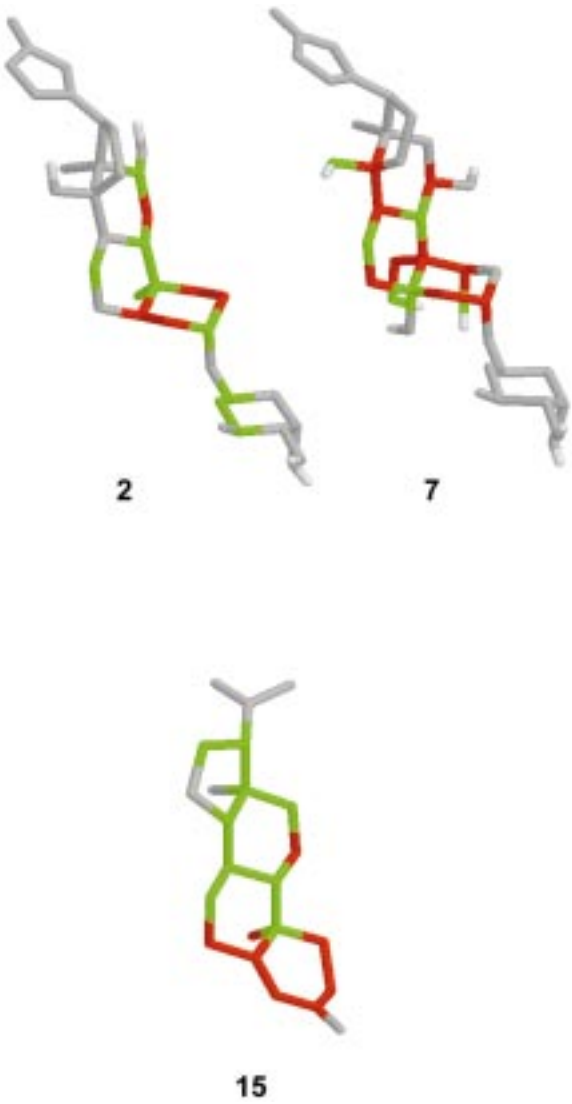

Figure 10. The structural parts of **2**, **7**, and **15** which are most responsible for the affinity to the cyclophane, **3**, cavity are marked in red (> 2.0 kcal/mol) and green (> 1.5 kcal/mol).

Ursodeoxycholic acid, **10**, also binds preferentially with the C/D-ring system (see Figure 8). The equatorial hydroxy group of ursodeoxycholic acid, **10**, at the B-ring does not lead to a repulsion but contributes to the interaction with the inside of the cyclophane tube (the cavity) with a small value of 0.3 kcal/mol (see Figure 8). Lithocholic acid, **11**, binds preferentially through the C/D rings, through the two methyl groups at the C/D junction and through the carboxylic acid side chain to the cavity (Figure 8). In addition to these cholic acid compounds, the two cortisone steroids, hydrocortisone, **12**, and cortisone, **13**, as well as testosterone, **14**, were docked into the cavity of cyclophane, **3**.

The lowest energy conformation of the hydrocortisone complex shows the highest interactions at the B/C/D-ring atoms (see Figure 9). In addition to the van der Waals interactions of the enone atoms of the A-ring, these two atoms show also attractive electrostatic interactions. The complex exhibits a hydrogen bond of the terminal hydroxy group at the alkyl side chain of the D-ring of **12** to a methoxy group of one benzene ring of the cyclophane **3** (distance 2.0 Å, O-H–O angle: 141°). Similar results as for hydrocortisone, **12**, were obtained for cortisone, **13** (see Figure 9). The same atoms as in **12** contribute in **13** to the highest interactions with the apolar cyclophane cavity. A hydrogen bond similar to that found in the

complex of **12** and **3** was found in the complex of **13** and **3** (distance 2.0 Å, O-H–O angle: 142°). Testosterone, **14**, binds preferentially through the A-, B-, and C-rings (see Figure 9). Nearly the entire steroid structure is encapsulated in a pitched conformation. Again an electrostatic contribution of the enone system to the attractive interactions could be determined. The highest interactions ($>$ 2.0 kcal/mol) are made by the A/B-ring junction atoms and those directly attached to them.

In an additional study, docking experiments were performed for three more steroids, digoxin, **2**, ouabain, **7**, and progesterone, **15**, (see Figure 10) to predict their binding modes. These structures are known to have high affinity to the antigen binding fragment of the 26-10 [2, 3, 7], the 40-50 [8], and the DB3 [6] antibodies.

Digoxin, **2**, is encapsulated by the cyclophane with most parts of the A-, B- and C-rings, the methyl group at the A/B-ring junction and the sugar moiety (see Figure 10). The highest interactions are made by the A-ring atoms. Ouabain, **7**, binds in a similar mode as digoxin, **2**, to the cyclophane cavity. It is encapsulated with most parts of the A-, B- and C-rings, the hydroxy groups attached to the A-ring and the C/D-ring junction, and the CH_2OH substituent (see Figure 10). Interactions of the sugar moiety and the receptor could not be found. Progesterone, **15**, is a smaller molecule than **2** and **7**. It binds with nearly the complete steroid skeleton. The orientation of the steroid inside the cavity is rather pitched (see Figure 10). The highest interactions are made by the A-ring atoms and two C-ring atoms.

Free energy calculations

The binding free energies were calculated for the steroid cyclophane complexes using the linear interaction energy approach. The desolvation energy will increase in the more polar solvent. This could lead to a certain divergence between the calculated and experimental $\Delta G_{binding}$. The calculated and experimental [4] free energies of binding are shown in Table 2. The α value for the calculation of the mean energy was found to be 0.31 to fit the data for compounds **4** and **8** to **11**, the saturated steroid structures. A large value of 0.52 of α was necessary to fit the data for compounds **12** to **14**, the unsaturated steroids.

The V_{vdw} and V_{elec} values are the ensemble-averaged van der Waals and electrostatic interactions between the host and the guest. The ensemble average is based on the trajectories of molecular dynamics simulation which are carried out separately in water and in the antibody.

The average values for the binding free energy give reasonable trends: the binding affinity increases slightly from cholic acid, **4**, to lithocholic acid, **11**, and from hydrocortisone, **12**, to testosterone, **14**. The mean unsigned divergence of the experimental and calculated value is 1.2 kcal/mol with the exception of compound **4**. This divergence corresponds well with the reported mean errors of binding free energy calculations by Åqvist et al. [24].

The solvent box in which the molecular dynamics calculations were performed consisted of water molecules only, in contrast to the experimental measurements of the binding free energies which were performed in a water/methanol mixture [4]. The desolvation energy will increase in the more polar solvent. This could lead to a certain divergence between the calculated and experimental $\Delta G_{binding}$.

The list of the predicted binding free energy values for compounds **2**, **7**, and **15**, for which no experimental data were available, is presented in Table 3.

Most important for binding are the apolar interactions of the surfaces of the steroids with the receptor cavity. Considering the substructures of the steroids making high contacts with the binding site of the receptor (Figures 8–10), the most important part of binding in each case is the steroid skeleton itself. The more hydroxyl groups are present on the steroid skeleton, the more polar the compound becomes and the better it is solvated in water. Based on this, the structures themselves can be divided into three major groups depending on the number of hydroxyl groups at the center of the steroidal skeleton (see Table 4). The calculated binding free energies are very similar to each other in each group.

Group 1 represents the highest binding free energies with the compounds having no OH groups at all. Compound **11** has a binding free energy of -5.2 kcal/mol, while **14** ($\Delta G^{calc}_{binding} = -5.7$ kcal/mol) and **15** ($\Delta G^{calc}_{binding} = -7.5$ kcal/mol) have even larger binding energies. Compounds **14** and **15** are tilted inside the cavity so that nearly the whole structure makes high contacts with the apolar cavity (see Figure 10). In contrast, the calculated binding mode of **11** is perpendicular to the cavity and a much smaller part of the structure interacts with the cavity. This may be the reason for the low binding free energy for compound **11**.

Table 2. Experimental [27] and calculated binding free energies for cyclophane, **3**, in kcal/mol

Compound	$\langle V^{elec}_{water} \rangle$	$\langle V^{elec}_{antib} \rangle$	$\langle V^{vdw}_{water} \rangle$	$\langle V^{vdw}_{antib} \rangle$	ΔG_{exp}	ΔG_{calc}
4	−73.9±0.3	−55.7±0.9	−26.0±0.2	−46.0±0.5	−2.9	2.8±1.1
8	−56.5±0.3	−55.4±0.2	−27.4±0.3	−47.0±0.0	−3.2	−5.6±0.9
9	−55.8±0.5	−52.0±0.1	−28.2±0.0	−46.4±0.2	−3.9	−3.8±0.9
10	−55.5±0.3	−54.1±0.8	−28.9±0.2	−43.7±1.1	−4.4	−3.9±0.7
11	−41.1±0.4	−39.0±0.4	−30.7±0.0	−46.3±0.0	−5.2	−3.9±0.9
12	−64.2±2.6	−52.0±1.2	−23.9±0.1	−45.5±0.0	−4.1	−5.0±3.9
13	−64.7±0.8	−52.3±2.5	−24.2±0.3	−40.7±0.5	−4.3	−2.2±2.4
14	−69.7±0.8	−66.1±1.1	−21.8±0.3	−36.4±0.2	−4.8	−5.7±2.1

Group 2 represents compounds with one OH group at the steroidal skeleton. The binding free energies in group 2 are lower than in group 1 and range from −3 kcal/mol to −5 kcal/mol experimentally, and from −4 kcal/mol to −6 kcal/mol computationally. Much of these steroids is buried in the receptor in these cases.

In group 3, all the compounds have two or more OH groups (**2**, **4** and **7**), the binding free energies are computed to be positive, and the complexation is an endergonic process. In the case of compound **4**, the measured free energy (−2.9 kcal/mol) is small and the hydroxyl group at the B-ring even leads to repulsion (see Figure 8). As shown in Figure 10, ouabain, **7**, binds with the A, B, and C-ring to the apolar cavity. This part of the structure of ouabain, **7**, has many polar substituents. These OH groups prevent a strong host–guest binding which results in a positive complexation free energy. However, it seems that during the linear response approximation of the binding free energies the polar-apolar repulsive interactions have been overestimated.

The binding affinities of steroids to the apolar cavity of the cyclophane decrease with an increasing number of polar substituents on the steroidal skeleton. Strong host–guest binding is based on van der Waals interactions between the guest and the host. In addition, the desolvation energy of the steroids is larger with increasing hydrogen-bonding sites.

Surface properties

To investigate similarities between physicochemical surface properties of the ligands a neural network approach was explored. (For computational details see the Appendix.)

The electrostatic potentials and hydrophobicities on the molecular surfaces of the ligands are investigated to determine whether there is a relationship with the affinities of the steroids to the artificial cyclophane receptor, **3**.

Cholic acid, **4**, was chosen as an example for describing in detail the nature of the Kohonen maps. Figure 11 presents the Kohonen maps of the *e*lectrostatic *p*otential (ESP) (top) and of the *hy*drophobicity *p*otential (HYP) (bottom) of **4**. In the ESP map the red areas indicate a strongly negative ESP and the purple areas high positive ESP values. The red areas in the HYP map stand for high hydrophilicity, whereas the purple or blue areas correspond to high hydrophobicity. The corresponding scaling of the ESP and the HYP ranges between the maximum and minimum value of the considered property for cholic acid, **4**, that is −46.89 kcal/mol up to 36.62 kcal/mol for the ESP and −0.01 up to 0.1 for the HYP.

Cholic acid, **4**, has four sites with a rather large negative value of the ESP, the three OH groups and the COOH group. The Kohonen map of the ESP shows four isolated regions with a red-yellow color in correspondence to these four sites. The carbonyl oxygen at the COOH group has the most negative ESP value and corresponds to the large red region at the right-hand side of the Kohonen map. The space between this group and the OH groups at the B- and C-rings is characterized by a rather apolar region, the D-ring without any polar substituents, which is represented by green colored regions in the map. High positive ESP values that correspond to the hydrogens of the OH groups are colored in purple.

The polar substituents, the OH group at the A-, B- and C-ring and the COOH group at the alkyl side chain of the D-ring, present strongly negative HYP values. These values represent regions of low hydrophobicity and are colored in red. The steroid skeleton, which is in general rather apolar and hydrophobic, is presented

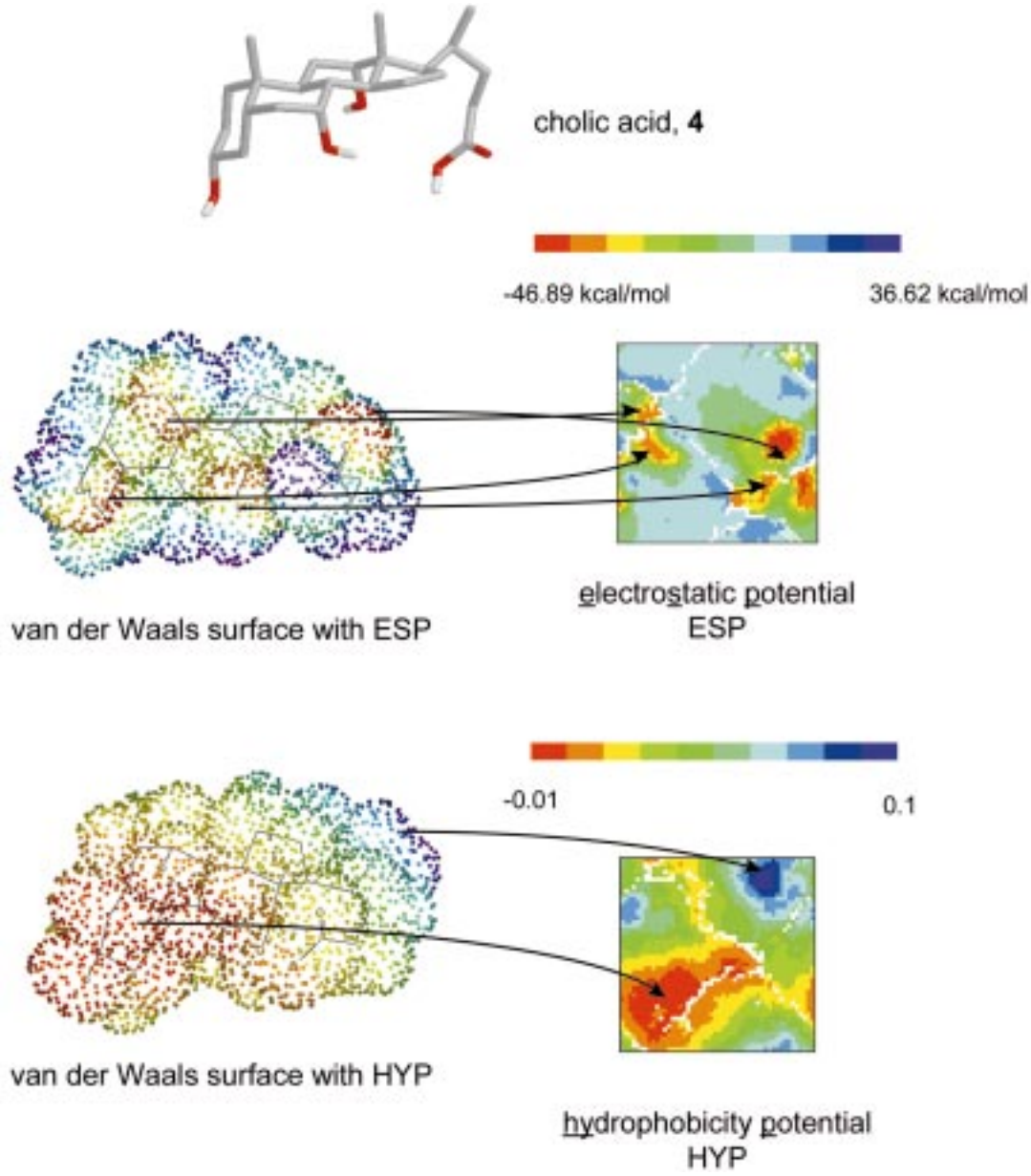

Figure 11. The electrostatic surface potential (ESP) and hydrophobicity potential (HYP) of cholic acid, **4**, projected onto the van der Waals surface and the corresponding Kohonen map. The values for the ESP are given in kcal/mol.

by blue, green, and purple regions at the top of the HYP map.

As the interactions between the receptor and the steroids are mostly apolar, we emphasize the importance of hydrophobicities and concentrate our study on this property in the following. Figure 12 presents the individual hydrophobicity maps of the steroids. For each structure a single network has been trained. The scaling of the HYP is the same for all of the 11 structures, in order to compare the structures with each other. The scaling ranges between the highest and lowest HYP value of the entire dataset. It can be clearly seen that e.g. ouabain, **7**, or digoxin, **2**, are not very hydrophobic, while progesterone is the most hydrophobic as indicated by the blue and magenta regions in the map.

The sequence of the maps in Figure 12 was chosen according to increasing affinity of the given steroid

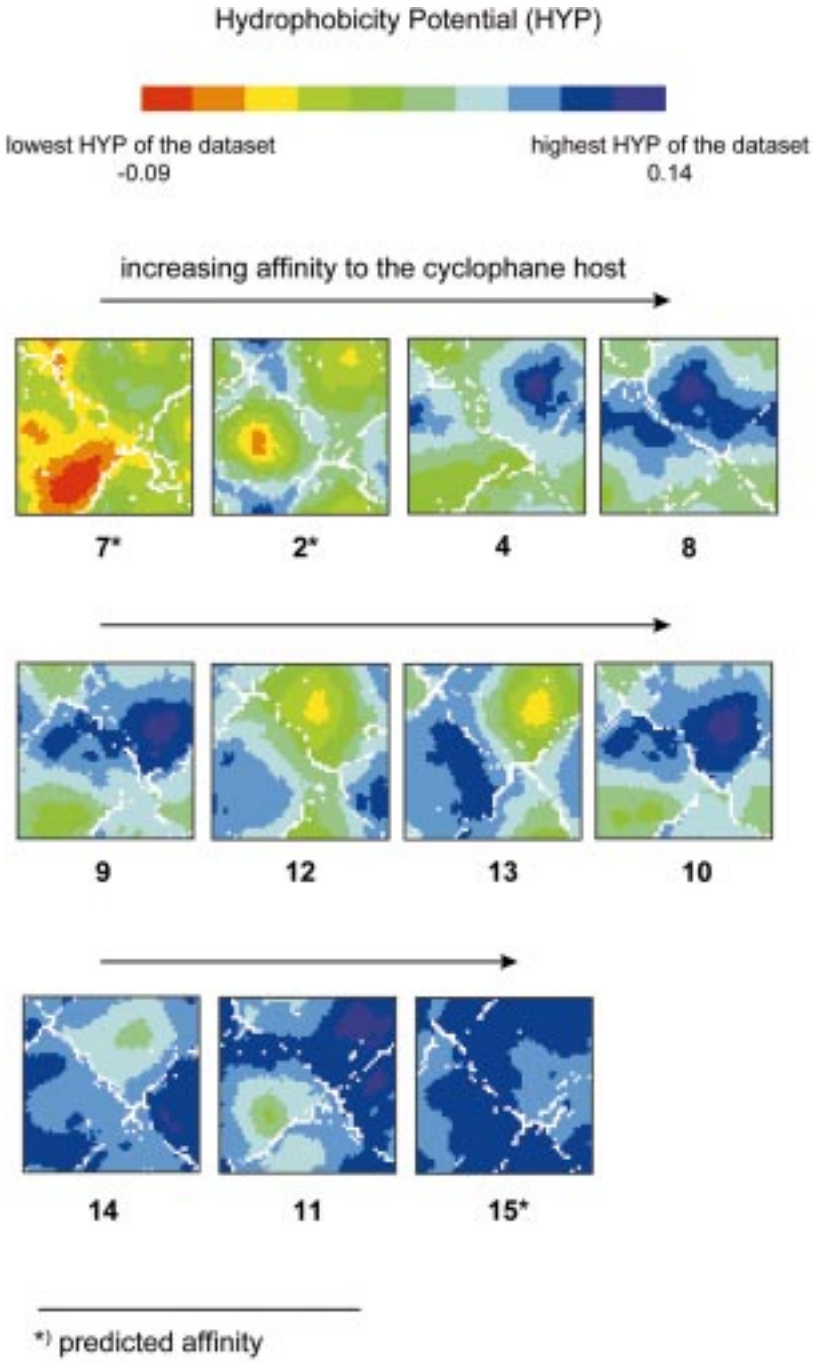

Figure 12. The hydrophobicity potential maps of **2**, **4**, and **7** to **15**. The scaling of the colors ranges between the lowest and highest HYP of the entire dataset. The sequence of the maps corresponds to an increasing affinity to the cyclophane host **3**.

Table 3. Predicted free binding energies $\Delta G_{binding}$ for the cyclophane, **3**, in kcal/mol

Compound	$\langle V^{elec}_{water} \rangle$	$\langle V^{elec}_{antib} \rangle$	$\langle V^{vdw}_{water} \rangle$	$\langle V^{vdw}_{antib} \rangle$	ΔG_{calc}
2	−92.3±1.8	−72.3±0.0	−35.5±0.1	−57.3±0.0	2.2±0.8
7	−131.6±1.3	−102.9±2.8	−32.2±0.2	−54.9±0.7	6.9±2.9
15	−32.3±0.2	−32.3±0.0	−28.0±0.0	−42.1±0.2	−7.3±1.3

Table 4. Three major groups of compounds dependent on the number of OH-groups at the steroidal skeleton. $\Delta G_{binding}$ for cyclophane, **3**, in kcal/mol

Group 1	Compounds				No OH-group
	11	**14**	**15**		
$\Delta G_{binding}$ (exp.)	**−5.2**	**−4.8**	–		
$\Delta G_{binding}$(calc.)	−3.6	−5.7	−7.3		
Group 2	Compounds				One OH-group
	8	**9**	**10**	**12**	
$\Delta G_{binding}$ (exp.)	**−3.2**	**−3.9**	**−4.4**	**−4.1**	
$\Delta G_{binding}$(calc.)	−5.6	−3.8	−3.9	−5.0	
Group 3	Compounds				≥ 2 OH-groups
	2	**7**	**4**		
$\Delta G_{binding}$ (exp.)	–	–	−2.9		
$\Delta G_{binding}$(calc.)	>0.0	>0.0	>0.0		

to the hydrophobic cyclophane based on the experimental ΔG values presented in [4]. In the case of compounds **7**, **2**, and **15**, the classification is based on the predicted affinities (see Table 3).

A quantitative value of the overall hydrophobicity of each structure was obtained from the number of neurons which represent hydrophobic areas. The size of the hydrophobic area is proportional to the number of the blue and purple neurons, those which have HYP values within the range of the last three segments of the coloring palette (HYP between 0.05 and 0.14). Therefore, the sum of the neurons colored in blue and purple is taken into account (see Table 5).

Table 5 gives the number of neurons corresponding to high hydrophobicity for each map shown in Figure 12. The affinity of the steroids to the cyclophane cavity correlates reasonably well with the number of hydrophobic neurons. Exceptions in this correlation are the compounds hydrocortisone, **12**, cortisone, **13**, and testosterone, **14**. They show an increasing affinity in agreement with an increasing number of hydrophobic neurons, but they do not fit the entire correlation. A possible reason could rest in the unsaturated steroid skeleton (see Figure 7) which leads to a different shape of the surface. However, altogether the correlation between the experimental and predicted receptor

Table 5. Number of neurons that represent hydrophobic areas (compounds in order of increasing affinity)

Compound	ΔG (kcal/mol)	Neurons
7*	6.9	0
2*	2.2	227
4	−2.9	536
8	−3.2	1105
9	−3.9	1121
12	−4.1	716
13	−4.3	1192
10	−4.4	1158
14	−4.8	1859
11	−5.2	1813
15*	−7.3	2363

*Predicted affinity.

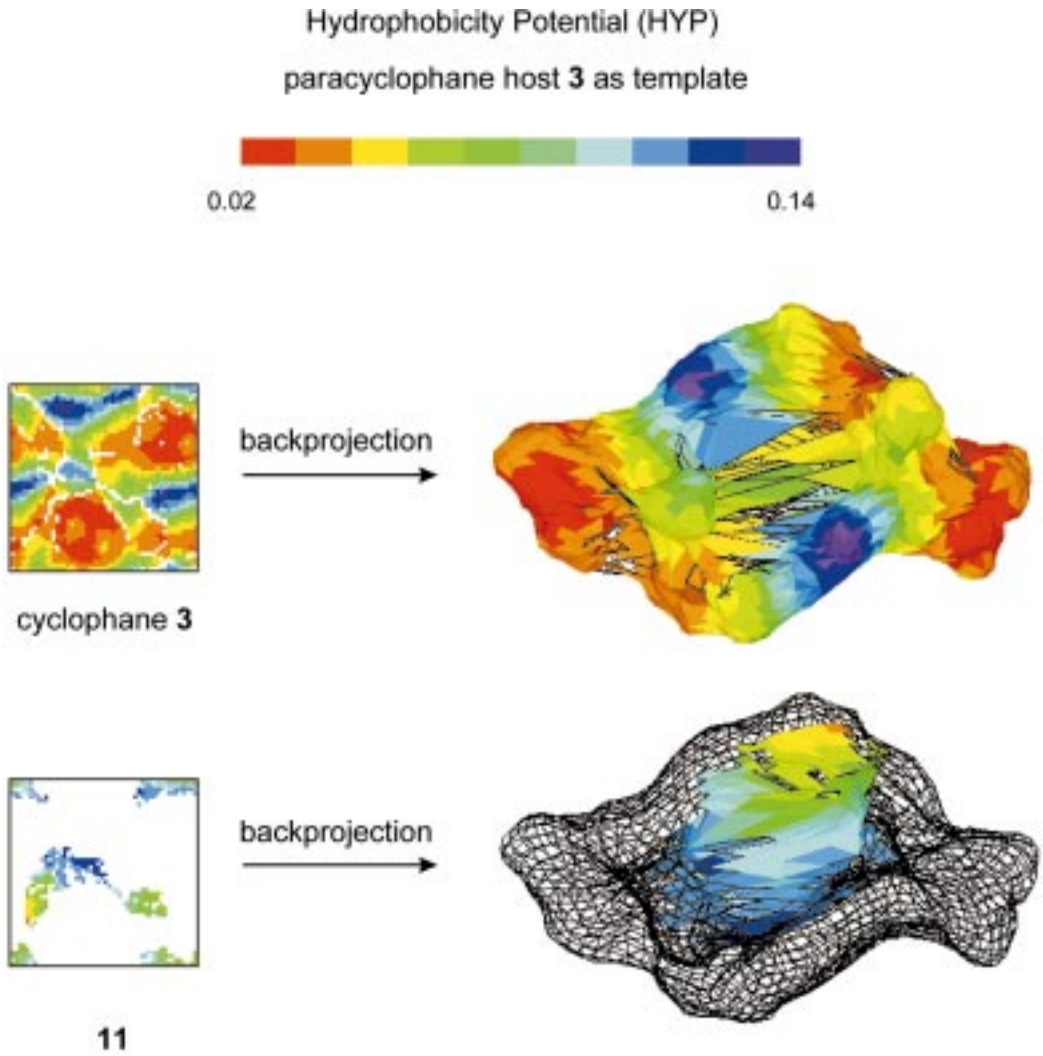

Figure 13. The backprojection of the Kohonen maps of the HYP of the host, **3** and the template map of **11** onto the molecular surface of **3**.

affinities is represented quite well by the number of neurons corresponding to hydrophobic regions.

The hydrophobic surface potentials of digoxin, **2**, and ouabain, **7**, in Figure 12 show that these are the most hydrophilic compounds with the lowest minimum value (HYP $= -0.09$) for the hydrophobicity potential. The yellow-red area in the map of digoxin, **2**, corresponds to the sugar moiety. The sugar moiety is the most hydrophilic part of the structure. This corresponds well with the experimental and calculated binding mode of digoxin, **2**, to the 26-10 antibody (Figures 3 and 5). The ligand binding domain of the antibody is rather apolar and the hydrophilic and polar sugar moiety is directly exposed to the solvent outside the cavity. The large red areas in the map of compound **7** present the three hydroxyl groups at the A-ring (see Figure 1) and the sugar moiety.

Figure 13 presents the backprojection of the Kohonen map obtained in the template approach ([36, 38, 39] and Appendix) onto the three-dimensional surface of the cyclophane receptor, **3**. The HYP ranges between the highest and lowest value of **3** and not of the entire dataset. First the backprojection of the hydrophobicity map of the cyclophane onto the surface of the cyclophane is shown (top of Figure 13). The shape of the cyclophane, **3**, can be perceived again. The only deviations that occur are due to the distortion of the torus during the projection process of the Kohonen mapping [42, 44].

The backprojection is an illustrative method to show the contact surface between the ligand (e.g., **11**) and the host, **3**. The map for lithocholic acid, **11**, obtained by the template approach can be projected back onto the three-dimensional surface of the template structure, **3** (bottom of Figure 13). Here, the template approach was to train a network with the coordinates of the host, **3**, and sending through the surface data of the guest, **11**. In areas of short distances or overlap of the surfaces of guest and host the mesh is colored (inner surface of the host, **3**), whereas non-contact surfaces are indicated by a black open mesh (outer surface of **3**). The HYP of **11** shows that the hydrophobic body of the ligand (blue and purple) lies inside the cyclophane, **3**, cavity and the hydrophilic areas (yellow and orange) are exposed to the solvent.

Conclusions

Our docking experiments show that antibodies recognize steroids in apolar hydrophobic pockets between the variable light and heavy chains. The dominant forces are hydrophobic desolvation and van der Waals interactions, rather than hydrogen bonds. The specificity and affinity arises mainly from shape complementarity. The calculated binding modes of the digoxin related steroids **2** and **4** to **7** show that the complementarity of the surfaces is closest between the lactone and the steroidal D-ring and decreases towards the periphery of the binding site.

The binding modes of cholic acid, **4**, and deoxycholic acid **8** show preferential encapsulation with parts of the A- and the B-ring. In contrast, **9** to **11** prefer the interaction with their C/D rings and parts of the carboxylic acid side chain at the D-ring. The two cortisones **12** and **13** as well as testosterone, **14**, are preferentially encapsulated with the A/B rings including the enone system in the apolar cyclophane cavity. Digoxin, **2**, and ouabain, **7**, are encapsulated with parts of the A-, B- and C-rings in the cyclophane receptor **3**. For digoxin, **2**, the polar sugar moiety shows weak interactions with the receptor, whereas for ouabain, **7**, the sugar moiety does not contribute to the binding affinity. Progesterone, **15**, has the highest interactions realized by the A-ring atoms.

The computed binding free energies to the cyclophane cavity (ΔG) agree well (mean divergence 1.2 kcal/mol) with experimental binding free energies of the steroid cyclophane complexes for **4** and **8** to **14**. The binding free energy calculations yield positive ΔG values for **7** and **2** and predict a very high affinity for the apolar progesterone, **15**. The presence of polar, highly solvated groups at the C- and B-rings of the steroid structure reduces the stability of the inclusion complexes formed with cyclophane, **3**.

Kohonen neural networks characterize progesterone, **15**, as the most hydrophobic and ouabain, **7**, as the most hydrophilic compound, respectively. The extent of the hydrophobicity correlates with the affinity of the steroids to the cyclophane receptor, **3**. For ouabain, **7**, and digoxin, **2**, the contact surfaces of the steroids are hydrophilic. Hence, physicochemical and structural properties, responsible for high receptor affinity, are similar for antibody or artificial receptor binding.

Appendix. Computational methods

Computational simulation of the antibody steroid binding modes

The structures of the steroids were minimized with the molecular modeling system MacroModel [14] using the MM3 force field [15]. The sequence of the antibody 26-10 was aligned with known highly homologous antibody structures in order to extract those parts of the light and heavy chain of the antibody which build the ligand binding domain. This sequence alignment was performed with the immunoglobin domain modeling program AbM [16].

The steroids were manually predocked into the ligand binding domain of the antibody with the InsightII/Discover [17] software package as well as by analyzing and visual inspection of the results.

Docking experiments to obtain the binding mode of the steroids in the antibody 26-10 were calculated using AutoDock [18]. This is an automated docking program which makes use of a Monte Carlo simulated annealing technique for exploration of the configurational space of the steroids inside the ligand binding domain of the antibody. The energy evaluation is performed by using grid based molecular affinity potentials. The charges for the electrostatic grid calculation of AutoDock were obtained from semiempirical PM3 VESPA charges calculated by the molecular modeling package VAMP [19]. For each AutoDock calculation of a binding mode 100 simulations were performed and each run consisted of 150 cycles, containing a maximum number of 8000 accepted and rejected steps. The initial annealing temperature was 500 K with a temperature reducing factor of 0.85 per cycle.

Computational simulation of the cyclophane steroid binding modes

Both the structures of the steroids and of the cyclophane, **3**, were obtained using continuous simulated annealing based on MM3 force field [15] calculations in the molecular modeling package MacroModel [14]. The annealing process was carried out from 300 K to 50 K. The cooling procedure was linear and continuous. First a 10 ps equilibration is performed at 300 K. Then in the course of the following 100 ps dynamic annealing simulations by cooling down the temperature slowly from 300 K to 50 K were done.

The binding modes of the steroids inside the cyclophane, **3**, were calculated using AutoDock [18] in the same way as described above, while treating the cyclophane, **3**, as a receptor.

Free energy calculation

Free energies of binding were calculated using a slightly modified Amber4.1 package [20]. The most accurate ways to calculate binding free energies are free energy perturbation or thermodynamic perturbation techniques [21–23]. The time to perform such calculations is substantial. However, Åqvist et al. introduced the linear interaction energy method to solve the free energy calculation problem [23, 24]. Åqvist expressed the free energy of binding by Equation 1:

$$\Delta G_{\text{binding}} = \frac{1}{2}\left(\left\langle V^{\text{elec}}_{\text{antibody}}\right\rangle - \left\langle V^{\text{elec}}_{\text{water}}\right\rangle\right) + \alpha\left(\left\langle V^{\text{vdw}}_{\text{antibody}}\right\rangle - \left\langle V^{\text{vdw}}_{\text{water}}\right\rangle\right) \quad (1)$$

ΔV_{elec} and ΔV_{vdw} are the electrostatic and the van der Waals potentials obtained from MD simulations for the ligand in water. The factor of $\frac{1}{2}$ is based on the linear response theory, while α is an empirical parameter that has to be determined for each specific receptor system. The method has been tested on various inhibitors of endothiapsenin which belongs to the family of aspartic proteinases [25]. Differences between calculated and experimental values of $\Delta G_{\text{binding}}$ of less than 1 kcal/mol have been found. The linear interaction energy approximation method has been implemented in the Amber4.1 package [20].

Atomic charges were derived from the electrostatic potential by performing Hartree-Fock calculations with a 6-31G* basis set within the Gaussian94 package [26] for both the ligands and the cyclophane receptor.

The simulations were carried out using the AMBER4.1 program package [20] with the use of the AMBER94 force field [27]. Both guest and host-guest complexes were embedded in a rectangular solvent box with about 800 water molecules for the guests and about 1300 water molecules for the complexes. Jorgensen's TIP3P model was used [28].

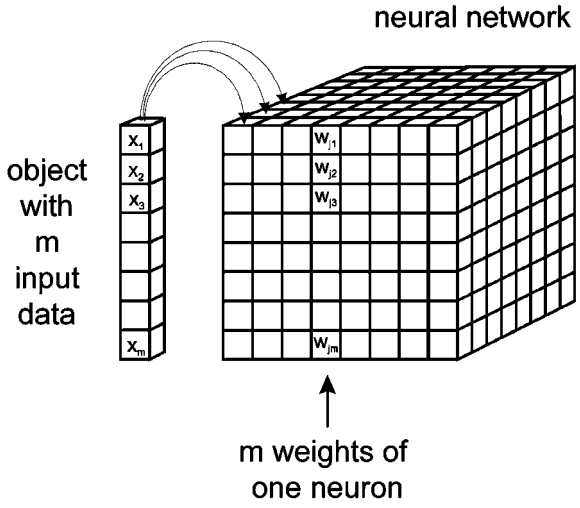

Figure 14. A schematic presentation of the architecture of a Kohonen neural network.

After initial energy minimization, molecular dynamics simulations consisting of 50 ps of equilibration and 80 ps of data collection were performed for each ligand, solvated in water as well as bound to a solvated receptor.

The simulations for both the guest and the host-guest complex were carried out in a TIP3P solvent box employing periodic boundary conditions at a constant pressure and temperature. The pressure and temperature were fixed at 1 atm and 300 K, respectively. The average value of the temperature was maintained by means of the Berendsen coupling algorithm [29]. The coupling constant to external heat was fixed at 0.2 ps^{-1}. All the simulations were performed at a nonbonded cutoff of 10.0 Å. The nonbonded pair list was updated every 12 steps. The time step for each simulation was set to 2 fs. The SHAKE procedure [29, 30] was applied to constrain all bond lengths to their equilibrium values.

Neural network approach

Artificial neural networks are able to process information and consist of many single units, the so-called neurons. The neurons are usually arranged in layers which communicate with each other [31–33]. The method used here is the self-organizing network

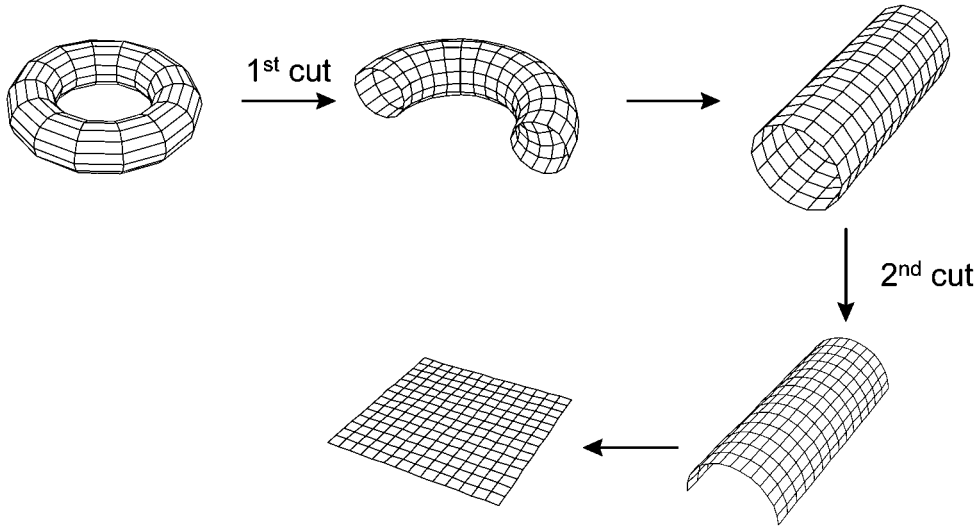

Figure 15. The toroidal shape of a Kohonen neural network. The Kohonen map is reached by two cuts of the original torus.

of Kohonen [34]. The network is able to recognize similarities between the input data and establish neighborhood relationships. Self-organizing Kohonen neural networks can be used to study data of high-dimensional spaces by projecting them into a lower-dimensional, usually two-dimensional, space [34]. Points adjacent in the high-dimensional space will be projected into adjacent points of the two-dimensional map.

Figure 14 shows the architecture of a Kohonen network: each column represents a neuron, and each box in such a column represents a weight of a neuron [33]. Each neuron has as many (m) weights, w_{ji}, as the dimension (m) of the input vector.

An object, with a certain input vector of dimension m, will be mapped into that neuron, that has weights most similar to the input vector values. The similarity index can be the Euclidean distance. The weights of each neuron will be adjusted but to a degree that decreases with increasing distance to the winning neuron.

The neurons can also be arranged on the surface of a torus (see Figure 15). In such a toroidal arrangement, each neuron has the same number of direct neighbors and there are no edge neurons. By cutting this torus twice, a two dimensional map is obtained (see Figure 15). This corresponds to a projection from a higher dimensional space into a two-dimensional map by keeping the topology of the input objects.

Observe that the two perpendicular cuts through the toroidal surface can be made at any arbitrary position. Hence, the maps in Figures 11–13 can be shifted or wrapped horizontally and vertically.

One important chemical application of Kohonen neural networks is the projection of three-dimensional molecular surfaces into two-dimensional maps [35–38] (see Figure 11). In this case, the input vector is of dimension three, corresponding to the x-, y-z-coordinates of the molecular surface. The maps are used to compare the surfaces with each other. Obviously, it is easier to compare two-dimensional maps than the three-dimensional molecular surface of a chemical compound [40, 41]. The Kohonen neural networks were generated and analyzed by the Kohonen Map Simulator KMAP [42].

The three-dimensional structure was taken from the binding mode obtained in the docking experiments using AutoDock. The van der Waals surfaces of these three-dimensional structures were calculated using the program SURFACE [43]. Both surface properties, the electrostatic potential and the hydrophobicity were calculated based on the partial atomic charges q_i of the compounds. These were obtained by the PEOE (Partial Equalization of Orbital Electronegativities) method [44, 45] and its extension to conjugated systems [46].

The molecular electrostatic potential (shown at the top of Figure 11) was calculated in a classical manner by moving a point charge of $+1e$ on the molecular surface and calculating the potential according to Coulomb's law from the partial atomic charges q_i [44]. It is summed over all single partial potentials in the

molecule (Equation 2).

$$V = \frac{1}{4\pi\epsilon_0} \sum_i \frac{q_i}{r_i} \quad (2)$$

r_i is the distance between the considered surface point and the atom i and V is given in [kcal/mol].

Several attempts have yet been made to define the relative lipophilicity values based on empirical investigations. These values can be obtained, e.g., from the partition coefficient (log P) of the sample in a polar/apolar reference system. Fujita et al. proved the additive-constitutive behavior of this partition coefficient. Hence, the hydrophobicity of a molecule can be given as a sum of partial lipophilicities, f_i, of i molecular fragments (Equation 3) [47].

$$\log P = \sum_i f_i . \quad (3)$$

A divergence occurs because of the neglect of the influence on log P of each fragment which is in the neighborhood of the considered fragment f_i. Heiden et al. introduced the calculation of the molecular lipophilicity potential (MLP) based on the subdivision of molecular lipophilicity into fragment contributions and projection of the lipophilicity onto the molecular surface (Equation 4) [48]. A distance dependent rule for the influence of different fragments on the lipophilicity at a surface point was thus developed,

$$MLP = \sum_i \frac{f_i}{1 + d_i} \quad (4)$$

where d_i is the distance of the considered point on the surface to the center of the fragment i in a three-dimensional space.

These surface properties, the electrostatic potential and the hydrophobicity potentials are calculated on the van der Waals surfaces, generated by the program SURFACE [43] and used as values for the coloring of the Kohonen maps.

The color scaling shown in Figure 11 stands for the highest and lowest obtained value of the electrostatic potential and the hydrophobicity of a sample compound. The arrows explicitly show which area of the surface has been projected into which region on the map.

Two approaches were applied to compare van der Waals surfaces of different molecules [36–38]. The first one is to train several networks, one with each single three-dimensional structure and to align the obtained maps according to structural features which can be recognized in the map. The second possibility is the template approach [38]. This approach requires an pre-alignment of the molecules of the dataset. Then, the network is trained once with the data of a template molecule, e.g., that one having the highest activity and every other structure is sent through this network. At regions of high similarity, colored areas appear on the corresponding map, whereas dissimilar regions are indicated by white areas.

Acknowledgements

We gratefully thank the ‘Fonds der Chemischen Industrie’ for financial support of the research stay of S.H. at the UCLA, and the National Science Foundation for the support of this research in the U.S.A. B.G. thanks the Alexander von Humboldt Stiftung for a scholarship.

References

1. Wallimann, P., Marti, T., Fürer, A. and Diederich, F., Chem. Rev., 97 (1997) 1567.
2. Jeffrey, D.P., Strong, R.K., Sieker, L.C., Chang, C.Y.Y., Campbell, R.L., Petsko, G.A., Haber, E., Margolies, M.N. and Sheriff, S., Proc. Natl. Acad. Sci. USA, 90 (1993) 10310.
3. Schildbach, J.F., Near, R.J., Bruccoleri, R.E., Haber, E., Jeffrey, P.D., Ng, S.-C., Novotny, J., Sheriff, S. and Margolies, M.N., J. Biol. Chem., 268 (1993) 21739.
4. Peterson, B.R., Wallimann, D.R., Carcanague, G. and Diederich, F., Tetrahedron, 51 (1995) 401.
5. Peterson, B.R., Mordasini-Denti, T. and Diederich, F., Chem. Biol., 2 (1995) 139.
6. Arevalo, J.H., Stura, E.A., Taussig, M.J. and Wilson, I.A., J. Mol. Biol., 231 (1993) 103.
7. Burks, E.A., Chen, G., Georgiou, G. and Iverson, B.L., Proc. Natl. Acad. Sci. USA, 94 (1997) 412.
8. Jeffrey, D.P., Schildbach, J.F., Chang, C.Y.Y., Kussie, P.H., Margolies, M.N. and Sheriff, S., J. Mol. Biol., 248 (1995) 344.
9. Gouverneur, V.E., Houk, K.N., Pascual-Teresa, de B., Beno, B., Janda, K.D. and Lerner, R.A., Science, 262 (1993) 204.
10. Kawakami, H., Yoshino, O., Odashima, K. and Koga, K., Chem. Pharm. Bull., 33 (1985) 5610.
11. a. Klärner, F.-G., Benkhoff, J., Boese, R., Burkert, U., Kamieth, M. and Naatz, U., Angew. Chem., 108 (1996) 1195.
    b. Klärner, F.-G., Benkhoff, J., Boese, R., Burkert, U., Kamieth, M. and Naatz, U., Angew. Chem. Int. Ed. Engl., 35 (1996) 1130.
12. Wallimann, P., Seiler, P. and Diederich, F., Helv. Chim. Acta, 79 (1996) 779.
13. Peterson, B.R. and Diederich, F., Angew. Chem., 106 (1994) 1688; Angew. Chem. Int. Ed. Engl., 33 (1994) 1625.
14. Mohamadi, F., Richards, N.G.J., Guida, W.C., Liskamp, R., Lipton, M., Canfield, C., Chang, G., Hendrickson, T. and Still, W.C., J. Comput. Chem., 11 (1990) 440.
15. Allinger, N.L., Yuh, Y.H. and Lii, J.-H., J. Am. Chem. Soc., 111 (1989) 8551.

16. a. Martin, A.C.R., Cheethan, J.C. and Rees, A.R., Proc. Natl. Acad. Sci. USA, 86 (1989) 9268.
b. Pederson, J., Searle, S., Henry, A. and Rees, A.R., Immunomethods, 1 (1992) 126.
17. InsightII/Discover, Biosym/Molecular Simulations Inc., San Diego, CA, USA.
18. a. Goodsell, D.S. and Olson, A.J., Proteins Struct. Funct. Genet., 8 (1990) 195.
b. Morris, G.M., Goodsell, D.S., Huey, R. and Olson, A.J., J. Comput.-Aided Mol. Design, 10 (1996) 293.
19. Rauhut, G., Alex, A., Chandrasekhar, J., Steinke, T., Sauer, W., Beck, B., Hutter, M., Gedeck, P. and Clark, T., VAMP Version 6.1, Erlangen, 1996.
20. Pearlman, D.A., Case, D.A., Caldwell, J.W., Ross, W.S., Cheatham III, T.E., Ferguson, D.M., Seibel, G.L., Singh, U.C., Weiner, P.K. and Kollman, P.A., Amber4.1, University of California, San Francisco, CA, 1995.
21. Gilson, K.M., Given, J.A., Bush, B.L. and McCammon, J.A., Biophys. J., 72 (1997) 1047.
22. Fox, T., Scanlan, T.S. and Kollman, P.A., J. Am. Chem. Soc., 119 (1997) 11571.
23. Lamb, M.L. and Jorgensen, W.L., Chem. Biol., 1 (1997) 449.
24. Åqvist, J., Medina, C. and Samuelsson, J.-E., Protein Eng., 7 (1994) 385.
25. Auterhoff, H., Knabe, J. and Höltje, H.-D., Lehrbuch der Pharmazeutischen Chemie, Wissenschaftliche Verlagsgesellschaft mbH, Stuttgart, Germany, 1994, p. 655.
26. Gaussian 94, Gaussian Inc., Pittsburgh, PA, USA.
27. Cornell, W.D., Ciepak, P., Bayly, C.I., Gould, I.R., Merz, K.M., Ferguson, D.M., Spellmeyer, D.C., Fox, T., Caldwell, J.W. and Kollman, P.A., J. Am. Chem. Soc., 117 (1995) 5179.
28. Jorgensen, W.L., Chandrasekhar, J., Madura, J.D., Impey, R.W. and Klein, M.L., J. Chem. Phys., 79 (1983) 926.
29. Berendsen, H.J.C., Postma, J.P.M., van Gunsteren, W.F., DiNola, A. and Haak, J.R., J. Chem. Phys., 81 (1984) 3684.
30. Ryckaert, J.P. and Ciccotti, G., J. Chem. Phys., 78 (1983) 7368.
31. Zupan, J. and Gasteiger, J., Anal. Chim. Acta, 248 (1991) 1.
32. Gasteiger, J. and Zupan, J., Angew. Chem., 105 (1993) 510; Angew. Chem. Int. Ed. Engl., 32 (1993) 502.
33. Zupan, J. and Gasteiger, J., Neural Networks in Chemistry and Drug Design, second edition, Wiley-VCH, Weinheim, Germany, 1999.
34. Kohonen, T., Biol. Cybern., 43 (1982) 59.
35. Gasteiger, J. and Li, X., Angew. Chem., 33 (1994) 671; Angew. Chem. Int. Ed. Engl., 33 (1994) 643.
36. Anzali, S., Barnickel, G., Krug, M., Sadowski, J., Wagener, M., Gasteiger, J. and Polanski, J., J. Comput.-Aided Mol. Design, 10 (1996) 521.
37. Handschuh, S., Schwab, C.H., Sadowski, J., Teckentrup, A., Wagener, M., Gasteiger, J., Levi, P., Will, T., Zell, A., Siemens, H., Klebe, G., Mietzner, T., Weber, F., Barnickel, G., Anzali, S. and Krug, M., In Fels, G. and Schubert, V. (Eds) Stepwise Database Screening as a Tool for Systematic Drug Development. Software Entwicklung in der Chemie 11, GDCh, Frankfurt, 1997, pp. 183–192.
38. Anzali, S., Gasteiger, J., Holzgrabe, U., Polanski, J., Sadowski, J., Teckentrup, A. and Wagener, M., In Kubinyi, H., Folkers, G. and Martin, Y.C. (Eds) 3D QSAR in Drug Design, Vol. 2, Kluwer/ESCOM, Dordrecht, 1998, pp. 273–299.
39. Polanski, J., Gasteiger, J., Wagener, M. and Sadowski, J., Quant. Struct.-Act. Relat., 17 (1998) 27.
40. Gasteiger, J., Li, X., Rudolph, C., Sadowski, J. and Zupan, J., J. Am. Chem. Soc., 116 (1994) 4608.
41. Gasteiger, J., Li, X. and Uschold, A., J. Mol. Graphics, 12 (1994) 90.
42. KMAP, Version 2.1, Li, X., Wagener, M. and Gasteiger, J., 1996.
43. SURFACE program, Version 1.0, Sadowski, J. and Gasteiger, J., 1994.
44. Li, X., Gasteiger, J. and Zupan, J., Biol. Cybern., 70 (1993) 189.
45. Gasteiger, J. and Marsili, M., Tetrahedron, 36 (1980) 3219.
46. Gasteiger, J. and Saller, H., Angew. Chem., 97 (1985) 699; Angew. Chem. Int. Ed. Engl., 24 (1995) 687.
47. Fujita, T., Iwasa, J. and Hansch, C., J. Am. Chem. Soc., 86 (1964) 5175.
48. Heiden, W., Moeckel, G. and Brickmann, J., J. Comput.-Aided Mol. Design, 7 (1993) 503.
49. The lowest energy binding mode in the complex of **3** with chenodeoxycholic acid, **9**, was not considered here, as the steroid structure is outside the cavity and bound by hydrogen bonds, which likely will be broken in polar solvents.